Eur. Phys. J. E **12**, 481–496 (2003)
DOI: 10.1140/epje/e2004-00020-9

THE EUROPEAN PHYSICAL JOURNAL E

Dynamics of living polymers

B. O'Shaughnessy[1,a] and D. Vavylonis[1,2,b]

[1] Department of Chemical Engineering, Columbia University, 500 West 120th Street, New York, NY 10027, USA
[2] Department of Physics, Columbia University, 538 West 120th Street, New York, NY 10027, USA

Received 11 February 2003 / Received in final form 23 September 2003
Published online 20 January 2004 –

Abstract. We study theoretically the dynamics of living polymers which can add and subtract monomer units at their live chain ends. The classic example is ionic living polymerization. In equilibrium, a delicate balance is maintained in which each initiated chain has a very small negative average growth rate ("velocity") just sufficient to negate the effect of growth rate fluctuations. This leads to an exponential molecular weight distribution (MWD) with mean $\bar{N}$. After a small perturbation of relative amplitude ϵ, e.g. a small temperature jump, this balance is destroyed: the velocity acquires a boost greatly exceeding its tiny equilibrium value. For $\epsilon > \epsilon_c \approx 1/\bar{N}^{1/2}$ the response has 3 stages: (1) Coherent chain growth or shrinkage, leaving a highly non-linear hole or peak in the MWD at small chain lengths. During this episode, lasting time $\tau_{\rm fast} \sim \bar{N}$, the MWD's first moment and monomer concentration m relax very close to equilibrium. (2) Hole-filling (or peak decay) after $\tau_{\rm fill} \sim \epsilon^2 \bar{N}^2$. The absence or surfeit of small chains is erased. (3) Global MWD shape relaxation after $\tau_{\rm slow} \sim \bar{N}^2$. By this time second and higher MWD moments have relaxed. During episodes (2) and (3) the fast variables $(\bar{N}, m)$ are enslaved to the slowly varying number of free initiators (chains of zero length). Thus fast variables are quasi-statically fine-tuned to equilibrium. The outstanding feature of these dynamics is their ultrasensitivity: despite the perturbation's linearity, the response is non-linear until the late episode (3). For very small perturbations, $\epsilon < \epsilon_c$, response remains non-linear but with a less dramatic peak or hole during episode (1). Our predictions are in agreement with viscosity measurements on the most widely studied system, α-methylstyrene.

PACS. 82.35.-x Polymers: properties; reactions; polymerization – 05.40.-a Fluctuation phenomena, random processes, noise, and Brownian Motion – 87.15.Rn Biomolecules: structure and physical properties; Reactions and kinetics; polymerization

1 Introduction

Living polymers are intriguing examples of soft matter and have major roles in technology and biology. The classic system, of major importance for the synthesis of high-grade polymer materials and the subject of a long history of fundamental experimental and theoretical study, is living anionic polymerization [1–25]. This class of polymerization is widely employed to manufacture polymers with nearly monodisperse MWDs and controlled architectures such as block and star copolymers [26]. A recent variant on this theme with immense potential technological impact is living free radical polymerization [27,28]. Other examples include worm-like surfactant micelles [29–36] and biological polymers such as actin and tubulin filaments [37–42] whose special properties are exploited by living cells for motility and structural integrity.

As polymeric or polymer-like materials, the unique feature of these systems is that the chains are dynamic objects, with constantly fluctuating lengths. When subjected to an external perturbation, they are able to respond dynamically via polymerization and depolymerization reactions allowing a new thermodynamic equilibrium to be attained. These systems are "living" in the sense that a change in their environment leads to a new equilibrium molecular weight distribution (MWD). All of this should be compared to conventional inert polymer materials whose MWDs are frozen.

The subject of this paper is the dynamical response of living polymers. We study the class of living polymers which is exemplified by living ionic polymerization, having the following characteristics: (i) monomers add and subtract from chain ends and (ii) the total number of chains is fixed. In the biological world, actin and microtubule filaments satisfy condition (i), and the dynamics of both filaments and filament caps are frequently described by situation (ii) [43]. Wormlike micelles on the other hand

[a] e-mail: bo8@columbia.edu
[b] e-mail: dv35@columbia.edu

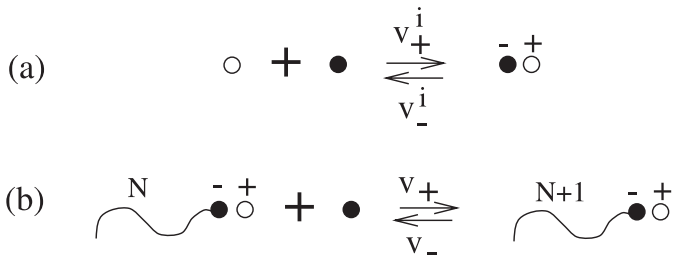

Fig. 1. (a) Schematic of initiation reaction in ionic polymerization. Empty (filled) circle represents initiator (monomer). (b) Polymerization and depolymerization reactions at the ionic chain end of a polymer chain of N units.

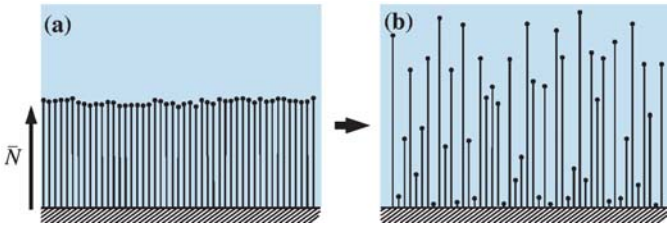

Fig. 2. Fluctuations of living polymer chain length in equilibrium are very large. For clarity, living chains are depicted as if extending from an imaginary substrate. Living ends are shown as filled circles. Even if one starts with a nearly monodisperse MWD as in (a) and with monomer concentration (grey background) such that polymerization and depolymerization rates balance, random polymerization and depolymerization reactions eventually broaden the distribution up to distances of the same order as the mean $\bar{N}$, as shown in (b). Note the resulting MWD includes chains of "zero" length (free initiators).

in some cases grow from their ends only [29,30] (condition (i)) but do not satisfy condition (ii): the number of micelles is not conserved. Interestingly, this makes their dynamical response very different (see discussion section).

Our presentation will focus on living ionic polymerization, though most of our results are completely general. In these systems, polymers grow reversibly from their ionic ends (see Fig. 1). Due to their "living" nature, if fresh monomer is added polymers will grow until the extra monomer has been consumed; further addition of a different monomer species, say, will resume polymer growth. The main achievement of this technique is a distribution of chain lengths with very small Poisson fluctuations around the mean. This monodisperse MWD is not however a true equilibrium distribution. For sufficiently long times slow depolymerization reactions become important and lead to a true equilibrium MWD which is in fact extremely broad. For many applications, for example styrene, the timescale to reach equilibrium is extremely large and depolymerization-induced broadening effects are unimportant [44]. However, in some cases equilibration times are accessible, an example being α-methylstyrene whose equilibrium properties have been studied in many experiments [2–13].

The reason that chain length fluctuations in equilibrium are so large is that even when a state is reached where the monomer concentration reaches a steady state value such that polymer growth rates exactly balance depolymerization, through polymerization and depolymerization reactions monomers continue to be reshuffled among living chains. Thus even if one starts with an essentially monodisperse MWD as shown in Figure 2a, random addition and subtraction of monomers from chain ends will result in a "diffusive" random walk motion of chain ends in N-space (where N is the number of monomer units added to initiator) with a certain characteristic "diffusivity" D. Since there is no restoring force to this motion, chain ends will eventually diffuse to distances of the same order as the mean chain length, resulting in a broad distribution as shown in Figure 2b. In a simple mean-field picture where monomer-monomer excluded volume interactions are neglected this leads to the Flory-Schultz equilibrium distribution [3,45,46]

$$\phi_\infty(N) = \frac{1}{\bar{N}_\infty} e^{-N/\bar{N}_\infty}, \tag{1}$$

where $\bar{N}_\infty$ is the equilibrium mean length.

The thermodynamic properties of equilibrium living polymers have been studied in a large number of experimental and theoretical works. According to theory, going beyond mean field by accounting for excluded-volume interactions leads to power law modifications [18–20,34] to equation (1). Moreover, an analogy [14–17] between a living polymer system and the much studied Ising spin system in the formal limit of spin dimensionality n becoming zero (similar to the well-known analogy in the thermodynamic theory of semidilute polymer solutions [47,48] which can in fact be formulated equivalently to a living polymer system [49]) showed that the polymerization phase transition near the polymerization temperature is second-order with a number of characteristic power-law exponents. The results of a large number of experiments by the group of Greer, measuring both the MWD itself [13] and other thermodynamic properties [2,4] are apparently consistent with the above theories, favoring somewhat the non mean-field approach.

The most essential feature of living polymers however, namely their ability to respond *dynamically* to external perturbations, remains largely unexplored. How does an equilibrium living polymer system respond to a small perturbation? A conceptually simple perturbation is the addition of a small amount of extra monomer (an "m-jump"). A similar perturbation, easier to perform in practice, is a "T-jump," i.e. a small sudden change in temperature. Under such a perturbation, how rapidly and in what manner will the monomer concentration, MWD and mean chain length reach a new equilibrium? In this paper we address these questions theoretically. We will compare our predictions in Section 8 with small T-jump viscosity relaxation experiments by Greer et al. [11]. This same group

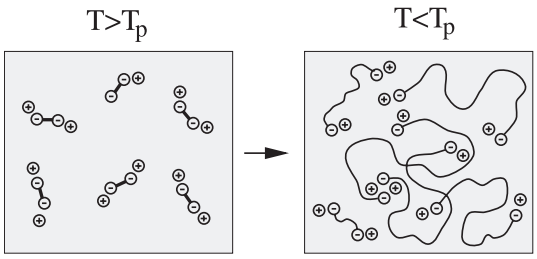

Fig. 3. Schematic of one of the classes of experiment performed by Greer's group [12,13]. The mix of monomer, initiator and solvent is stored for sufficiently long above the polymerization transition temperature T_p such that all initiator is activated. At this point all living chains are of "zero" length; we refer to these as "free initiators" (bifunctional dimers in this case). After a quench below T_p, polymerization onsets and the system's response to abrupt temperature changes is then studied. In this paper we study more elementary perturbations: very small T-jumps of an already equilibrated system.

has also monitored monomer and MWD dynamics following much stronger perturbations, finite temperature quenches [12,13] (see Fig. 3).

Our main broad conclusion is that, counter-intuitively, the response to a very small perturbation is extremely strong: even though the initial and final MWDs (the latter attained after relaxation is complete) are very close to one another, the MWD at intermediate times is very strongly perturbed from equilibrium, i.e. its shape is very different from either the initial or final equilibrium shapes. In this sense, there are no small perturbations: a small thermodynamic perturbation well-described by a linear susceptibility (i.e. one inducing a small change in the equilibrium state) has nonetheless a large dynamical effect; intermediate states deviate strongly from equilibrium in the sense that observables are perturbed in a highly non-linear manner. We refer to this as dynamical ultrasensitivity.

A hint of this sensitivity is already apparent in equilibrium, where a very delicate balance is established between growth and shrinkage such that the net polymerization velocity v is essentially zero, of order $1/\bar{N}_\infty$ (due to the small fraction of special non-depolymerizable chains of length $N = 0$). Now the effect of a small T-jump (say) is to produce a small but finite velocity which overwhelms this tiny velocity value and destroys the delicate balance sustaining equilibrium. Thus if for example v becomes positive, the MWD will *uniformly translate* toward larger molecular weights, creating a depletion in the MWD at small chain lengths, as shown schematically in Figure 4. This translation process stops only after sufficient monomer has been polymerized such that the monomer concentration drops close to its destination equilibrium value, corresponding to a recovery of the zero net growth rate equilibrium condition. We find that only on a much longer timescale does "diffusion" of chain ends fill up the hole and lead the system to the destination equilibrium MWD, as shown in Figure 4.

Why does this hole develop in the MWD? The reason is that chain length scales homogenized by diffusion, $(Dt)^{1/2}$, are smaller than scales affected by translational motion, vt, for times longer than the timescale $t^* \approx D/v^2$. Thus if t^* is shorter than the timescale needed for translation to stop, a depletion hole develops in the MWD. But even when translation is completed earlier than t^*, we find that the perturbation is still nonlinear; even though no hole is formed there is still a large amplitude reduction in the MWD, much larger than the relative magnitude of the initial perturbation, ϵ.

This work is related to earlier theory of Miyake and Stockmayer [44] who, following a prior treatment by Brown and Szwarc [50], studied analytically and numerically the dynamics in the special case where initially all monomer is unpolymerized (see Fig. 5). Their analytical results, applicable in the case of very small depolymerization rates, showed a 2-stage relaxation. During the first, lasting a time $\sim \bar{N}_\infty$, living chains grow coherently from zero length up to the equilibrium value. In the second stage the shape of the sharply peaked MWD relaxes slowly toward the equilibrium exponential distribution. Although their perturbation analysis broke down during this stage, Miyake and Stockmayer estimated that its duration scales as $\bar{N}_\infty^2$. Later theoretical studies addressed the second stage dynamics [51–53] of this special case.

A short announcement of the present work has already appeared [54]. The structure of the paper is as follows. In Section 2 we establish the dynamical equations obeyed by living polymers which show the nonlinear coupling between the monomer population and the living chain MWD. For simplicity, we neglect excluded volume interactions and chain length dependent polymerization rates. Starting from the equations of Section 2 we then analyze the response to a T-jump. This response depends on the sign of the velocity induced by the perturbation. The case of positive initial velocity is analyzed in Sections 3 and 4, while the negative in Section 5. The special case of very small T-jumps is analyzed in Section 6. In Section 7 we show that the results of the previous sections directly generalize to small perturbations of arbitrary form. Finally we conclude with a discussion of the results, and the experimental outlook.

2 Living polymer dynamics: monomer-polymer coupling

An important aspect of living polymers dynamics is the coupling between the two distinct species present in the solution, free monomers and living chain MWD: on the one hand living chain growth rates depend on the concentration of free monomer and on the other hand, due to mass conservation, monomer concentration is a function of the living chain MWD. Stated differently, living chains grow according to a velocity field which is self-consistently updated depending on the response of the MWD. In this section we develop the equations obeyed by monomer and MWD. The dynamical response to perturbations is discussed in the following sections.

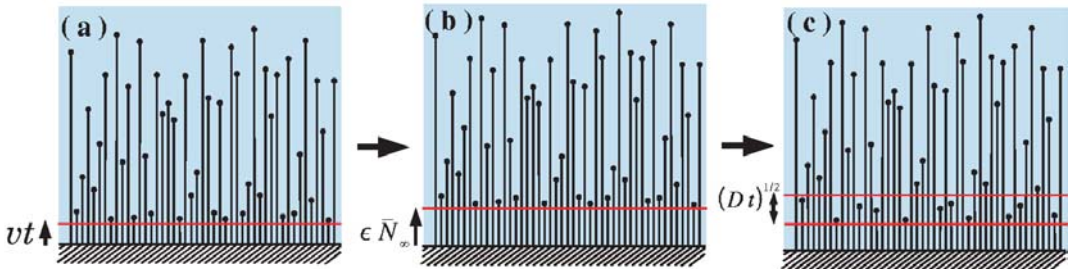

Fig. 4. There are three stages in the relaxation of living polymers to equilibrium. During the first, living polymers grow coherently as in (a). The translation stops when they have consumed enough monomer such that monomer concentration drops to a value for which polymerization and depolymerization balance (shown in (b)). During the second stage, (c), through "diffusive" random polymerization and depolymerization reactions, the MWD slowly fills the depletion of chains of short lengths. The third and final stage entails global shape relaxation of the MWD on a diffusion timescale corresponding to $\bar{N}_\infty$.

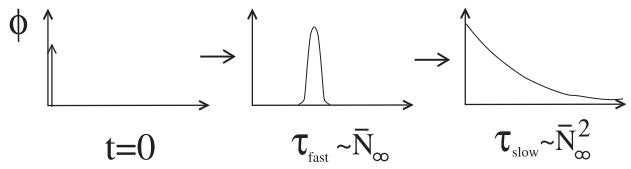

Fig. 5. Schematic of the MWD dynamics as analyzed by Miyake and Stockmayer [44] and their theoretical predictions regarding the timescales involved. (a) Initially ($t = 0$) all initiators are unpolymerized. (b) For $t \ll \tau_{\rm fast}$ chains grow coherently with a narrow MWD until its peak reaches the equilibrium mean length $\bar{N}_\infty$ at times of order $\tau_{\rm fast}$. (c) During a third stage lasting up to $\tau_{\rm slow}$, which was beyond their theoretical analysis, the MWD spreads to the equilibrium MWD.

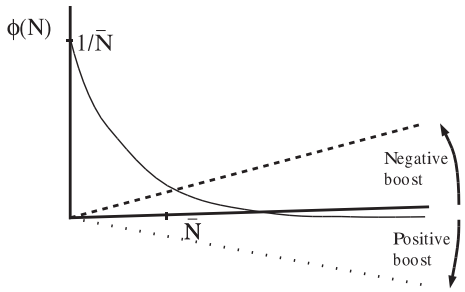

Fig. 6. Living polymer dynamics are equivalent to diffusion in a potential with slope $-v_t$. In equilibrium the slope reaches a very small value of order $1/\bar{N}_\infty$ (solid line) resulting in a broad MWD. Under a small T-jump the slope is strongly perturbed and depending on the direction of the jump becomes either positive (dashed line) or negative (dotted line).

A crucial feature of the living polymer systems we study is that the number of living chains remains fixed. This is what arises in the experiments of Greer et al. [2–4], where this number is determined by the amount of initiator initially added in the solution. Denoting i_0 the concentration of living chains (i.e. chains which have been initiated), mass conservation implies that monomer concentration, m_t, and MWD, $\phi_t(N)$, (t denotes time) obey

$$m_t = m_{\rm tot} - i_0 \bar{N}_t, \qquad \bar{N}_t \equiv \int_0^\infty dN\ N\ \phi_t(N), \quad (2)$$

where $m_{\rm tot}$ is the total monomer concentration (including polymerized monomers), and $\bar{N}_t$ is mean chain length. Here ϕ_t is normalized to unity and $N = 0$ corresponds to free initiator. The coupling between monomer concentration and the MWD is manifest in equation (2).

Now the dynamical equations equations obeyed by ϕ_t are

$$\frac{\partial \phi_t(N)}{\partial t} = -\frac{\partial j_t(N)}{\partial N},$$
$$j_t(N) \equiv v_t \phi_t(N) - D_t \frac{\partial \phi_t(N)}{\partial N}, \quad j_t(0) = 0, \quad (3)$$

where

$$v_t \equiv k^+ m_t - v^-, \qquad D_t \equiv (k^+ m_t + v^-)/2. \quad (4)$$

Here k^+ is the propagation rate constant and v^- is the depolymerization rate. The "diffusion" coefficient D_t, describes fluctuations in the rate of polymerization/depolymerization. Equation (3) is identical to the diffusion dynamics of a particle in a linear potential with time-dependent slope $-v_t$ whose time-dependent diffusion coefficient is D_t (see Fig. 6). The novelty here is that due to the coupling between the MWD and monomer, both the slope and diffusivity are functionals of ϕ itself.

The reflecting boundary condition in equation (3) at $N = 0$ represents the fact that when a living chain looses all of its monomers and becomes a free initiator molecule (i.e. reaches length $N = 0$) it cannot depolymerize further and must grow again. Now we restate equation (3) as

$$\frac{\partial \phi_t}{\partial t} = -v_t \frac{\partial \phi_t}{\partial N} + D_t \frac{\partial^2 \phi_t}{\partial N^2}, \quad \phi_t(0)/\phi_t'(0) = D_t/v_t, \quad (5)$$

where $\phi_t' \equiv \partial \phi_t / \partial N$.

Now it might at first seem that despite the coupling of equation (2), the monomer subsystem would effectively uncouple from the MWD dynamics, since one might naively expect that the monomer dynamics do not depend on the shape of the polymer MWD but only on the number of living chains. This would imply simple first order kinetics for m_t resulting in exponential relaxation of

the monomer concentration, independent of the MWD dynamics. The coupling however arises from the existence of special chains in the MWD of zero length, i.e. free initiator molecules of which there are $\phi_t(0)$, which unlike all other chains cannot depolymerize. Indeed, the dynamics obeyed by m_t, or equivalently v_t, are

$$\frac{dv_t}{dt} = -\frac{v_t}{\tau_{\rm fast}} - \frac{D_t\phi_t(0)}{\tau_{\rm fast}}, \quad \tau_{\rm fast} \equiv \frac{f}{rv^-} \approx \frac{f\,\bar{N}_\infty}{(1-f)v^-}. \quad (6)$$

We see clearly that the only aspect of the living MWD which monomers see is $\phi_t(0)$. Equation (6) is derived by calculating $d\bar{N}_t/dt$ by multiplying equation (3) by N, integrating over all N, using the reflecting boundary condition, and then using equation (2). The relationship between $\tau_{\rm fast}$ and $\bar{N}_\infty$ follows from equation (8) below. Here we have introduced the two basic independent dimensionless parameters of the system:

$$f \equiv \frac{v^-}{k^+ m_{\rm tot}}, \qquad r \equiv \frac{i_0}{m_{\rm tot}}. \quad (7)$$

The physical meaning of f is the following: if the system were a pure solution of unpolymerized monomer (plus solvent and initiator) f would be the ratio of backward to forward polymerization velocities. The value of f is temperature dependent, being unity at the polymerization temperature and smaller or larger than unity in the polymer and non-polymer phase, respectively. The parameter r, namely the ratio of living chain to total monomer concentration, is independent of temperature and is always much smaller than unity. Its smallness is related to the mean degree of polymerization being much larger than unity in equilibrium (see Eq. (8) below).

Now setting the time derivative in equation (5) to zero and using equation (2) it is shown in Appendix A that in equilibrium the Flory-Schultz distribution of equation (1) is recovered and one has to leading order in r:

$$\bar{N}_\infty \approx \frac{1-f}{r}, \quad \frac{m_\infty}{m_{\rm tot}} \approx f, \quad v_\infty \approx -\frac{v^-}{\bar{N}_\infty}, \quad D_\infty \approx v^-, \quad (8)$$

where $r \ll 1$ and subscript ∞ denotes the $t \to \infty$ equilibrium value for the corresponding variable. We assumed $(1-f)/r^{1/2} \gg 1$, i.e. that the temperature is not extremely close to the polymerization temperature.

An important feature in equation (8) is that in equilibrium the velocity, i.e. the slope of the "potential" term in equation (5), settles down to a very small negative value. Were there no diffusion, living chains subject to a negative velocity field would shrink to zero length. However due to the small magnitude of the velocity, diffusion is strong enough to broaden the MWD up to distances of order $\bar{N}_\infty$, as illustrated in Figure 2. We show in the following section that any apparently small external perturbation has an enormous effect on the velocity which, depending on the direction of the perturbation, may become either very negative or very positive.

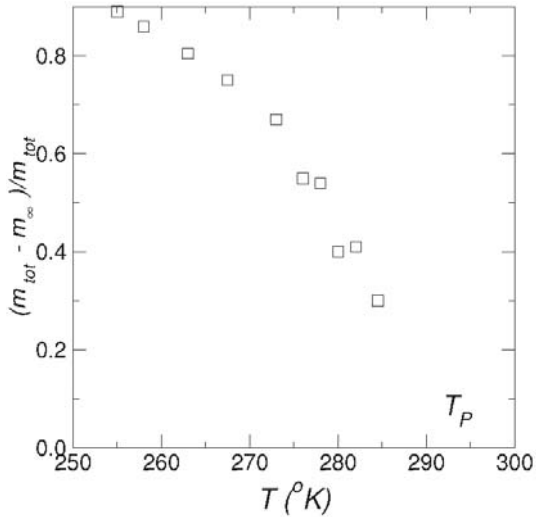

Fig. 7. Fraction of polymerized monomer in equilibrium as a function of temperature for living α-methylstyrene in tetrahydrofuran solvent, initiated by sodium napthalene. Data from reference [8]. Ratio of mole fraction of total monomer, $m_{\rm tot}$, to initiator is 0.0044. Mole fraction of total monomer is 0.1538. The polymerization temperature $T_{\rm p}$ is near 295 °K.

3 Response to T-jump; positive velocity boost

Perhaps the simplest way to perturb an equilibrium living polymer system is by a small temperature change (T-jump). Taking as an example α-methylstyrene, the data of Figure 7 show equilibrium fraction of polymerized monomer as a function of temperature; evidently, changes in T lead to different values of the equilibrium monomer concentration m_∞ and therefore of $\bar{N}_\infty$ as well. In this section we consider relaxation dynamics after an equilibrated system is subjected at $t = 0$ to a small temperature change δT such that the system will eventually reach new equilibrium values m_∞ and $\bar{N}_\infty$. That is, we follow the dynamics of the transition from an old equilibrium towards a slightly different new equilibrium state.

The magnitude of the perturbation is measured by the small parameter

$$\epsilon \equiv \frac{\delta m_0}{m_\infty}, \quad (9)$$

where we define $\delta m_t \equiv m_t - m_\infty$ and similarly for other quantities. All equilibrium values refer to the destination ($t = \infty$) equilibrium values. Thus δm_0 is the initial ($t = 0$) deviation from the final equilibrium.

The value of ϵ is related to the magnitude of the T-jump. For example in the case of α-methylstyrene, assuming that the system is initially below the polymerization temperature T_p in the region of Figure 7 between 260 °K and 280 °K, one has using equation (9)

$$\epsilon \approx -\frac{\delta T}{50\ ^\circ{\rm K}} \qquad (\alpha\text{-methylstyrene}). \quad (10)$$

Thus for α-methylstyrene a temperature increase, $\delta T > 0$, results in a negative δm_0, i.e. a reduced initial

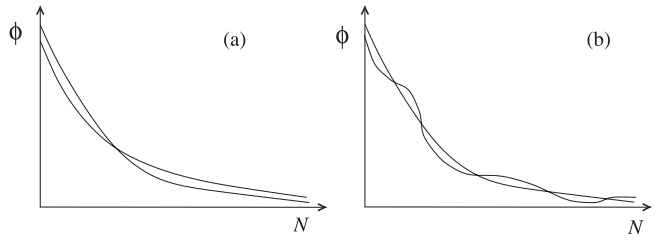

Fig. 8. (a) Sketch of the initial and final MWDs during a T-jump experiment. Both distributions are exponential. Though very close to one another, in the course of relaxation the time-dependent MWD becomes very different to the final exponential MWD. (b) General perturbation (non-exponential initial MWD). Most T-jump results derived here apply to this general case also.

monomer concentration relative to the destination equilibrium value.

Now the $t = 0$ relative perturbation of the MWD is

$$\frac{\delta\phi_0(N)}{\phi_\infty(N)} \approx \frac{\partial\phi_\infty(N)}{\partial\bar{N}_\infty}\frac{\delta\bar{N}_0}{\phi_\infty(N)} = \frac{\epsilon}{\theta}\left(1 - \frac{N}{\bar{N}_\infty}\right), \theta \equiv \frac{1-f}{f}. \tag{11}$$

This is of order ϵ and smaller than unity for all N (apart from the unimportant values $N \gg \bar{N}_\infty$ where the MWD is exponentially small) as shown in Figure 8a.

Because velocity, monomer concentration and mean chain length are all linearly related (see Eqs. (2, 8) and (4)) changes in these quantities are simply related as

$$\frac{\delta m_t}{m_\infty} \approx -\theta\frac{\delta\bar{N}_t}{\bar{N}_\infty} \approx 2\frac{\delta D_t}{D_\infty} \approx \frac{\delta v_t}{v^-}. \tag{12}$$

These relations are true for all times. They allow us to follow the dynamics of velocity alone. Once v_t is known, $\bar{N}_t$, m_t, D_t are determined.

From equations (12) and (9) the initial relative changes in v, D are:

$$\frac{\delta v_0}{v_\infty} \approx -\epsilon\,\bar{N}_\infty, \qquad \frac{\delta D_0}{D_\infty} \approx \frac{\epsilon}{2}. \tag{13}$$

The important point is that since $\bar{N}_\infty \gg 1$, the relative change in v is much larger than ϵ: the velocity is highly perturbed, as shown in Figure 6. Depending on the sign of ϵ, the velocity may remain negative as in equilibrium, or it may change sign. Since the relative perturbation in D is by contrast small, we see that the delicate velocity-diffusion balance which sustained equilibrium is now destroyed.

We will show below that relaxation to equilibrium now occurs in three stages. During the first, dominated by translational motion, the MWD is boosted far from its equilibrium shape. The next stage involves diffusive restoration of the region of the MWD which suffered maximum distortion during the first stage. The third and final episode entails a very slow diffusion-dominated recovery of the global MWD. For the remainder of this section we treat the case of a positive initial velocity boost, where chains initially grow ($\delta T < 0$ for α-methylstyrene). Negative velocity boosts, where chains initially shrink, are considered in Section 5.

3.1 Coherent chain growth: hole development

During the first stage of the relaxation process, velocity dominates over diffusion since v has been so strongly perturbed. Chains thus grow coherently, consuming the excess monomer in a timescale $\tau_{\rm fast}$ by which time translation will have halted and a highly non-linear hole will have developed in the MWD (see Fig. 9). Here $\tau_{\rm fast}$, defined in equation (6), is the time for the MWD to translate distance $\delta\bar{N}_0$ and reach the destination mean, i.e. $\tau_{\rm fast} \approx \delta\bar{N}_0/\delta v_0$ (see Eqs. (9, 13) and using Eq. (8)).

To see all of this more quantitatively, consider the velocity dynamics equation (6). Initially, the velocity term on the rhs is much larger in magnitude than the diffusion term. We show in Appendix B that this remains true up until a time $\tau_{\rm qs}$, defined below. It follows that for these times v_t relaxes exponentially. The same is true of $m_t, \bar{N}_t$ and D_t which we recall are linearly coupled to v_t (see Eq. (12)). Thus

$$\delta v_t \approx \epsilon\, v^-\, e^{-t/\tau_{\rm fast}} - v_\infty \quad (t \ll \tau_{\rm qs} = \epsilon\bar{N}_\infty^{3/2}\theta^{-3/2}/v^-). \tag{14}$$

Note that for $t \gg \tau_{\rm fast}$ there are no free initiators (at much longer times these are restored, see below). Thus for these intermediate times all chains are identical as far as on and off monomer kinetics are concerned, and the net rate of monomer-polymer mass exchange can only vanish if v_t vanishes. For this reason v_t decays to zero, though much later it will recover its small negative equilibrium value. The ϕ_t dynamics, equation (5), thus simplify to

$$\frac{\partial\phi_t}{\partial t} \approx -\epsilon\, v^- e^{-t/\tau_{\rm fast}}\frac{\partial\phi_t}{\partial N} + D_\infty\frac{\partial^2\phi_t}{\partial N^2} \qquad (t \ll \tau_{\rm qs}) \tag{15}$$

where the diffusion coefficient may be approximated by D_∞ since the contribution of δD_t is negligible (see Appendix B). This linear equation, plus the time-dependent boundary condition of equation (5), has solution

$$\phi_t(N) \approx \int_0^\infty dN'\, G_t^{\rm tran}(N, N')\phi_0(N') \qquad (t \ll \tau_{\rm qs}) \tag{16}$$

which describes a translating and simultaneously broadening MWD, as shown in Figure 9. Here $G_t^{\rm tran}(N, N')$ is the propagator of equation (15) whose properties are calculated in Appendix B.

An important quantity in what follows is $\phi_t(0)$, i.e. the concentration of free initiators. Using equation (16) we show in Appendix B that

$$\phi_t(0)/\phi_\infty(0) \approx \begin{cases} 1 - C\,(t/t^*)^{1/2} & (t \ll t^*) \\ F\,(t^*/t)^{3/2}e^{-t/t^*} & (t^* \ll t \ll \tau_{\rm fast}) \end{cases} \qquad t^* \equiv \frac{4D_\infty}{v_0^2}, \tag{17}$$

where $C = 4/\pi^{1/2}$ and $F = \pi^{-1/2}$. Equation (17) has a clear physical meaning: as the MWD translates, the position of its peak at $N = 0$ after time t has shifted to chain lengths of order $v_0 t$. Were diffusion absent, this would have created a depletion region in the MWD at small chain

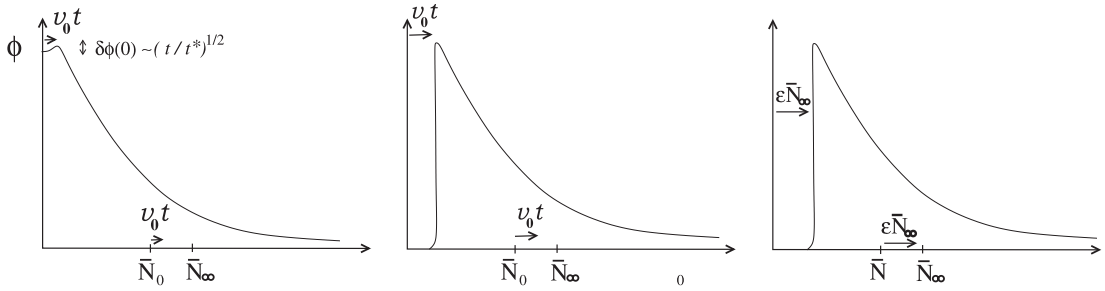

Fig. 9. Initial response of the MWD after a positive boost, case of strong perturbation ($t^* \ll \tau_{\rm fast}$). (a) For small times, chain end "diffusion" smooths out the hole which would otherwise form at small N due to chain growth. (b) At larger times coherent chain growth beats diffusion and a hole develops in the MWD. (c) Coherent growth stops when mean chain length reaches a value very close to $\bar{N}_\infty$, displaced by an amount $\epsilon\bar{N}_\infty/\theta$ from the original value $\bar{N}_0$. For typical cases, the parameter θ is of order unity.

lengths. However diffusion smooths out inhomogeneities on distances of size $(D_\infty t)^{1/2}$. Hence for times shorter than the crossover time t^* for which $v_0 t^* \approx (D_\infty t^*)^{1/2}$, diffusion has enough time to fill the translationally induced hole and the relative deviation from equilibrium is small. For times longer than t^* however, the MWD translates a distance away from the origin much larger than what diffusion could have homogenized, a hole develops in the MWD, and the concentration of zero length chains becomes exponentially small.

In equation (17) we assumed that the perturbation is large enough such that $t^* \ll \tau_{\rm fast}$. The special case of extremely small perturbations where this is no longer true is discussed separately in Section 5.

3.2 Diffusive length relaxation: hole filling

For times $t \gg \tau_{\rm fast}$ the fast variables monomer and mean chain length have relaxed very close to their equilibrium values. We have seen that velocity becomes exponentially small. Meanwhile (see below) the number of free initiators $\phi_t(0)$ is gradually recovering. At a certain moment, therefore, the 2 terms on rhs of equation (6) become equal to one another and we show in Appendix B that for all later times the velocity time derivative is much smaller. Hence the velocity dynamics are now fundamentally changed. The new regime is one of quasi-static evolution, enslaved to the dynamics of $\phi_t(0)$:

$$\delta v_t \approx \; -v^- \delta\phi_t(0) \qquad (t \gg \tau_{\rm qs}). \tag{18}$$

Physically, this reflects the fact that the the only aspect of the MWD shape seen by monomers is the amount of special non-depolymerizing zero-length chains. We see that as the MWD slowly rearranges itself, so the fast variables v_t, m_t and $\bar{N}_t$ variables respond quasi-statically.

Notice that the quasi-static regime does not onset after $\tau_{\rm fast}$ but rather after $\tau_{\rm qs}$. The reason is that during the initial boost the term $D_t\phi_t(0)$ in equation (6) decays exponentially on a timescale t^*; its magnitude therefore at $\tau_{\rm fast}$ is much smaller than v_t which decays on a timescale $\tau_{\rm fast}$ (see Eqs. (14) and (17)). There is thus a cross-over period before the quasi-static balance between the two terms is established.

Now let us examine the MWD dynamics. Since v_t becomes exponentially small after the MWD stops translating, we have

$$\frac{\partial\phi_t}{\partial t} \approx D_\infty \frac{\partial^2\phi_t}{\partial N^2} \qquad (\tau_{\rm fast} \ll t \ll \tau_{\rm fill}) \tag{19}$$

with reflecting boundary conditions at the origin. Here once again the contribution of δD_t is negligible (see Eqs. (12, 18), and (21)) and the corresponding term has been neglected in equation (19). Here

$$\tau_{\rm fill} \equiv \epsilon^2\,\theta^{-2}\,\tau_{\rm slow}, \qquad \tau_{\rm slow} \equiv \frac{\bar{N}_\infty^2}{4D_\infty}. \tag{20}$$

The timescale $\tau_{\rm slow}$ is the longest relaxation time of the system, the time for the slow global shape characteristics of the MWD to relax. It equals the diffusion time for the MWD width $\bar{N}_\infty$. Meanwhile $\tau_{\rm fill}$ is the diffusion time for the hole width, $\epsilon\bar{N}_\infty/\theta$. It is shown in Appendix B that equation (19) has solution

$$\frac{\phi_t(0)}{\phi_\infty(0)} \approx H\left(\frac{t}{\tau_{\rm fill}}\right)^{1/2} e^{-\tau_{\rm fill}/t} \qquad (\tau_{\rm fast} \ll t \ll \tau_{\rm fill}) \tag{21}$$

where $H = \pi^{-1/2}$. Thus for times shorter than $\tau_{\rm fill}$ the concentration of zero length chains remains exponentially small while for longer times the hole fills (see Fig. 10) and $\phi_t(0)$ recovers its equilibrium value.

3.3 Linearized dynamics at long times

For times beyond $\tau_{\rm fill}$ the hole-filling is complete and the MWD's non-linear feature has disappeared. Thus, finally, a truly linear regime onsets: relative deviations of all variables from equilibrium are less than unity and

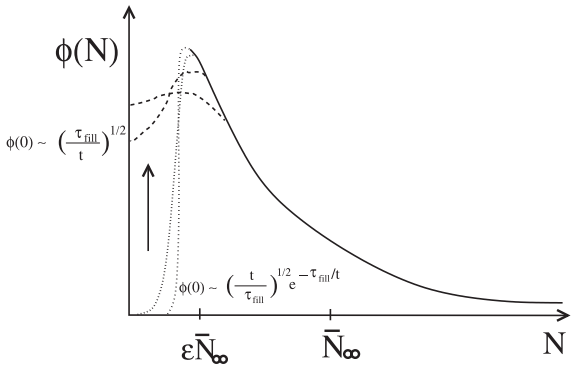

Fig. 10. Schematic of MWD during hole-filling episode. Dotted (dashed) lines show MWD profile for times $\tau_{\rm fast} \ll t \ll \tau_{\rm fill}$ ($\tau_{\rm fill} \ll t \ll \tau_{\rm slow}$).

perturbation theory can now be applied. This is done in Appendix C where we find

$$\frac{\delta v_t}{v^-} \approx -\delta\phi_t(0) \approx \begin{cases} J\,\phi_\infty(0)\,(\tau_{\rm fill}/t)^{1/2} & (\tau_{\rm fill} \ll t \ll \tau_{\rm slow}) \\ M\,\epsilon\phi_\infty(0)(t/\tau_{\rm slow})^{-3/2}e^{-t/(16\tau_{\rm slow})} & (t \gg \tau_{\rm slow}) \end{cases} \tag{22}$$

where J, M are positive constants of order unity. Thus $\delta\phi_t(0)$, and all of the fast variables which remain quasi-statically enslaved to $\phi_t(0)$, relax exponentially on a timescale $\tau_{\rm slow}$ with a power law prefactor.

4 The second moment of the MWD relaxes more slowly than the first

A picture has emerged of fast mass-related variables which relax in $\tau_{\rm fast}$ and slow MWD shape properties which relax in the much longer time $\tau_{\rm slow}$. The MWD's first moment defines the total mass in the polymer system: this is a fast variable and was considered in Section 3. The simplest slow shape property is the dispersion Δ_t,

$$\Delta_t \equiv \overline{N_t^2} - \bar{N}_t^2, \qquad \overline{N_t^2} \equiv \int_0^\infty dN\, N^2\phi_t(N), \tag{23}$$

which is closely related to the second moment. In this section we consider the very different and slow relaxation of this quantity.

Substituting equation (11) in equation (23) one finds that following a T-jump the initial relative perturbation in the dispersion, $\delta\Delta_0$, is

$$\frac{\delta\Delta_0}{\Delta_\infty} = -2\,\frac{\epsilon}{\theta}, \qquad \Delta_\infty = \bar{N}_\infty^2, \tag{24}$$

where the equilibrium value, Δ_∞, is found using equation (1). Now the dynamics of the dispersion can be derived by evaluating the time derivatives of $\overline{N_t^2}, \bar{N}_t$ in equation (23). These can in turn be calculated by multiplying equation (5) by N^2 and N, respectively, integrating over all N and using the boundary condition of equation (3). One has

$$\frac{1}{\Delta_\infty}\frac{d\delta\Delta_t}{dt} = \frac{1}{2\tau_{\rm slow}}\frac{D_t}{D_\infty}\left[1 - \frac{\bar{N}_t}{\bar{N}_\infty}\frac{\phi_t(0)}{\phi_\infty(0)}\right] \approx -\frac{1}{2\tau_{\rm slow}}\frac{\delta\phi_t(0)}{\phi_\infty(0)}. \tag{25}$$

Here we replaced D_t and $\bar{N}_t$ with their $t = \infty$ values. This is correct to leading order since the relative perturbations in these quantities are much smaller than that of $\phi_t(0)$ which undergoes much larger changes (see Sect. 3).

Now integrating equation (25) using equations (17, 21) and (22) one finds that up to the time $\tau_{\rm fill}$ the dispersion has changed very little relative to its value just after the perturbation at $t = 0$:

$$\frac{\Delta_t - \Delta_0}{\Delta_\infty} \approx \begin{cases} (C/3)(t/\tau_{\rm slow})(t/t^*)^{1/2} & (t \ll t^*) \\ t/(2\tau_{\rm slow}) & (t^* \ll t \ll \tau_{\rm fill}). \end{cases} \tag{26}$$

This is in stark contrast to the first moment which had already relaxed by the much shorter time $\tau_{\rm fast}$. The dispersion's relaxation process does not properly get going until times of order $\tau_{\rm slow}$:

$$\frac{\delta\Delta_t}{\Delta_\infty} \approx \begin{cases} \delta\Delta_0/\Delta_\infty + J\epsilon\theta^{-1}(t/\tau_{\rm slow})^{1/2} & (\tau_{\rm fill} \ll t \ll \tau_{\rm slow}) \\ \alpha\,\epsilon\,(t/\tau_{\rm slow})^{-5/2}e^{-t/(16\tau_{\rm slow})} & (t \gg \tau_{\rm slow}) \end{cases} \tag{27}$$

where $\alpha = 8M/39$. The relative perturbation in the dispersion remains of order ϵ for $t \ll \tau_{\rm slow}$ and subsequently relaxes exponentially.

5 Response to T-jump; negative velocity boost

In this section we study the case opposite to Section 3, when $\epsilon < 0$ and the T-jump induces a higher equilibrium monomer concentration and a smaller $\bar{N}_\infty$ (see Eq. (9)). Such a perturbation in the example of α-methylstyrene would be produced by an increase in temperature as one may see in Figure 7. In this case the sign of the initial perturbed velocity (Eq. (13)) is negative (see Fig. 6). Thus initially the MWD is not boosted towards larger molecular weights as in Section 3, but is instead boosted in the opposite direction, towards *smaller* N. Therefore, instead of depletion, an excess of small length chains and free initiators is produced, creating instead of a hole, a sharp peak in the MWD near $N = 0$ as shown in Figure 11.

Despite the differences between the two cases, many of the results of Section 3 remain unchanged. In fact all equations of Section 3 up to equation (16) remain unchanged, the only difference being that ϵ is negative. Thus equation (16) now describes a MWD coherently shrinking and simultaneously broadening with diffusion coefficient D_∞. But since free initiators cannot depolymerize, excess polymer must build up near $N = 0$. Indeed, starting from

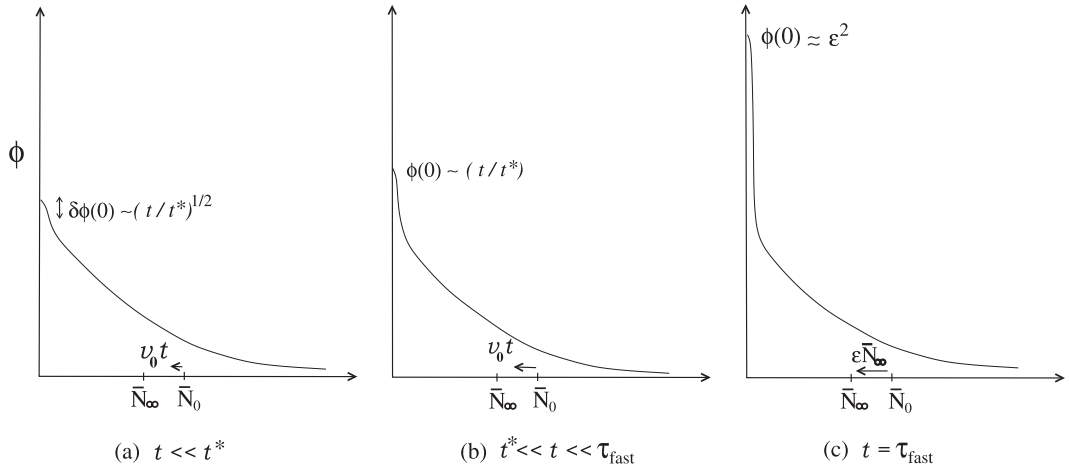

Fig. 11. Initial response of MWD after a negative boost (strong perturbation, $t^* \ll \tau_{\rm fast}$). (a) Chains shrink coherently and MWD moves from the initial mean $\bar{N}_0$ towards $\bar{N}_\infty$. For small times, diffusion smooths out excess peak at small N. (b) Beyond t^* diffusion is too slow to counteract coherent chain shrinkage and short chains accumulate at the origin. (c) Coherent shrinkage halts when mean chain length approaches $\bar{N}_\infty$.

equation (16) it is shown in Appendix D that

$$\frac{\phi_t(0)}{\phi_\infty(0)} \approx \begin{cases} 1 + C'\,(t/t^*)^{1/2} & (t \ll t^*) \\ F'\,(t/t^*) & (t^* \ll t \ll \tau_{\rm fast}) \end{cases} \tag{28}$$

where $C' = 4/\pi^{1/2}$ and $F' = 4$. Equation (28) has a similar interpretation to equation (17). For $t \ll t^*$ diffusion is fast enough to smooth out the excess polymer accumulated by the negative velocity at the origin and thus $\phi_t(0)$ remains close to its initial value (see Fig. 11a). For $t \gg t^*$ however the flow towards the origin is faster than what diffusion can smear out and a peak forms whose height increases with time, as shown in Figure 11b. (Once again it is assumed that the perturbation is not so small that $t^* \ll \tau_{\rm fast}$; the opposite case is examined in Sect. 5.)

After the completion of the first stage at times of order $\tau_{\rm fast}$, similarly to Section 3, the fast $m_t, \bar{N}_t$ variables have essentially relaxed and start to respond quasistatically to the slow diffusion-driven shape changes of the MWD. In fact we show in Appendix D that equations (14) and (18) still apply, but now with a different crossover timescale, $\tau_{\rm qs} = \tau_{\rm fast} \ln \bar{N}_\infty$. This difference arises because unlike the positive boost case $\phi_t(0)$ does not become exponentially small and so needs less time to catch up with the v_t term in the velocity dynamics, equation (6).

Similarly to the positive boost, equation (19) still applies for $t < \tau_{\rm fill}$. By this time the accumulation at the origin is able to diffuse to distances of the same size as the region from which it was transferred from during the first stage. Hence $\phi_t(0)$ becomes of order its initial value, and thereafter perturbation theory is valid. In Appendix D we show that

$$\phi_t(0)/\phi_\infty(0) \approx \begin{cases} K'(\tau_{\rm fill}/t)^{1/2} & (\tau_{\rm fast} \ll t \ll \tau_{\rm fill}) \\ 1 + J'(\tau_{\rm fill}/t)^{1/2} & (\tau_{\rm fill} \ll t \ll \tau_{\rm slow}) \\ 1 + M'\epsilon\,(t/\tau_{\rm slow})^{-3/2} e^{-t/(16\tau_{\rm slow})} & (t \gg \tau_{\rm slow}) \end{cases} \tag{29}$$

where K', J', and M' are positive constants of order unity. Note there is apparently no smooth cross-over at $t = \tau_{\rm fast}$ between the forms of equations (28) and (29). This is because there is in fact an extra episode at times of order $\tau_{\rm fast}$ during which the very thin peak spreads from width $(D_\infty t^*)^{1/2}$ to a width $(D_\infty \tau_{\rm fast})^{1/2}$. Note also that the time behavior for $t \gg \tau_{\rm fill}$ has been derived using the linearized dynamics of Appendix C.

Finally, to obtain the dispersion dynamics we use equations (28) and (29) in equation (25) to obtain

$$\delta\Delta_t/\Delta_\infty - \delta\Delta_0/\Delta_\infty \approx \begin{cases} -(C'/3)(t/\tau_{\rm slow})(t/t^*)^{1/2} & (t \ll t^*) \\ (-F'/4)(t/\tau_{\rm slow})(t/t^*) & (t^* \ll t \ll \tau_{\rm fast}) \\ -K'\epsilon\theta^{-1}(t/\tau_{\rm slow})^{1/2} & (\tau_{\rm fast} \ll t \ll \tau_{\rm fill}) \\ -J'\epsilon\theta^{-1}(t/\tau_{\rm slow})^{1/2} & (\tau_{\rm fill} \ll t \ll \tau_{\rm slow}) \\ -\delta\Delta_0/\Delta_\infty - (8M'/39)\,\epsilon\,(\tau_{\rm slow}/t)^{5/2} e^{-t/(16\tau_{\rm slow})} & (t \gg \tau_{\rm slow}) \end{cases} \tag{30}$$

which is very similar to equations (26) and (27) for the positive boost case. Again the dispersion relaxes on a timescale $\tau_{\rm slow}$, much longer then the relaxation time of $\bar{N}_t$.

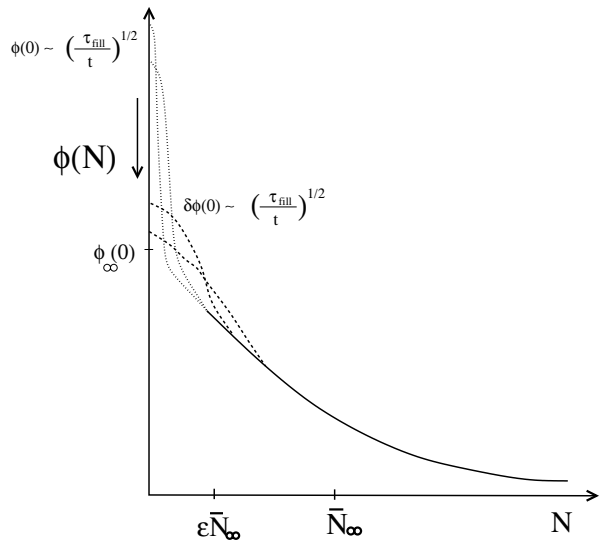

Fig. 12. Schematic of MWD development during $\tau_{\rm fast} \ll t \ll \tau_{\rm slow}$ when the small chain peak spreads diffusively. Dotted (dashed) lines correspond to times $\tau_{\rm fast} \ll t \ll \tau_{\rm fill}$ ($\tau_{\rm fill} \ll t \ll \tau_{\rm slow}$).

6 Very small T-jumps: ϵ less than its critical value $\epsilon_{\rm c}$

Hitherto we implicitly assumed sufficiently strong velocity boosts that the timescale t^* after which translational motion dominates diffusion and a hole or peak begins to form is shorter than the time for full development of the hole or peak, namely $\tau_{\rm fast}$. Now the ratio of these timescales is

$$\frac{t^*}{\tau_{\rm fast}} \approx \left(\frac{\epsilon_{\rm c}}{\epsilon}\right)^2, \qquad \epsilon_{\rm c} \equiv \frac{\theta^{1/2}}{\bar{N}_\infty^{1/2}}, \tag{31}$$

which defines a critical value of the perturbation parameter, $\epsilon_{\rm c}$. Clearly, the system's response must be different for ϵ values below this rather small threshold. We consider such very small perturbations in this section. Although a full hole or peak does not have time to develop, we will find that the response is still strong and non-linear.

Since such weak perturbations do not involve the creation of a complete hole or a peak in the MWD, one expects that the timescales t^* and $\tau_{\rm fill}$ associated with the their creation and destruction lose their physical meaning as cross-over timescales. This is shown in Appendix E where, using similar arguments to the ones of Sections 3 and 5, it is proved that weak perturbations are identical to stronger perturbations except that the regime up to t^* is truncated at $\tau_{\rm fast}$ and the following regime (which for stronger perturbations lasted till $\tau_{\rm fill}$) deleted. In Appendix E it is shown that for both positive and negative boosts, one has for the fast variables

$$\frac{\delta v_t}{v^-} \approx \begin{cases} \epsilon\, e^{-t/\tau_{\rm fast}} & (t \ll \tau_{\rm fast}) \\ -\delta\phi_t(0) & (\tau_{\rm fast} \ll t) \end{cases}. \tag{32}$$

Note that that the timescale $\tau_{\rm qs}$ does not appear since its magnitude lies between those of t^* and $\tau_{\rm fill}$.

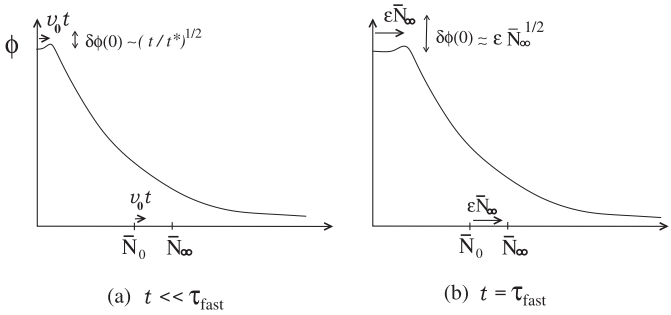

(a) $t << \tau_{\rm fast}$ (b) $t = \tau_{\rm fast}$

Fig. 13. Weak perturbations, $\epsilon < \epsilon_{\rm c}$. For such small perturbations $t^* \gg \tau_{\rm fast}$. (a) The coherent component of chain growth shifts the MWD mean towards $\bar{N}_\infty$. Diffusion is dominant, smoothing depletion at small N. The net effect is a nonlinear deviation from equilibrium. (b) By $\tau_{\rm fast}$ coherent growth halts, when mean chain length approaches $\bar{N}_\infty$. The behavior for longer times, $t \gg \tau_{\rm fast}$, is essentially the same as that shown by the dashed lines in Figure 10.

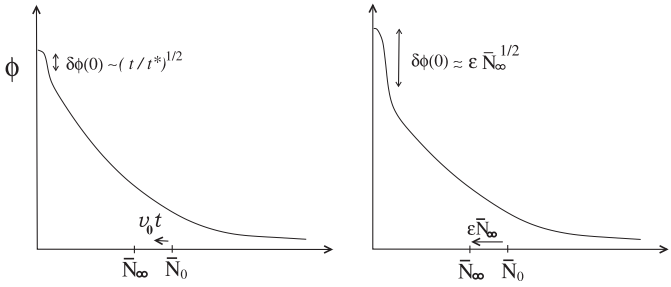

(a) $t << \tau_{\rm fast}$ (b) $t = \tau_{\rm fast}$

Fig. 14. As in Figure 13 but now for a negative initial velocity boost; a peak is formed instead of depletion. Evolution for $t \gg \tau_{\rm fast}$ as dashed lines of Figure 12.

The evolution of the MWD (see Figs. 13, 14) is similarly shown in Appendix E to lead to the following solution for $\phi_t(0)$ in the case of a positive initial velocity:

$$\frac{\phi_t(0)}{\phi_\infty(0)} \approx \begin{cases} 1 - C\,(t/t^*)^{1/2} & (t \ll \tau_{\rm fast}) \\ 1 - Q\,(\tau_{\rm fill}/t)^{1/2} & (\tau_{\rm fast} \ll t \ll \tau_{\rm slow}) \end{cases} \qquad (v_0 > 0) \tag{33}$$

while for a negative initial velocity one has instead

$$\frac{\phi_t(0)}{\phi_\infty(0)} \approx \begin{cases} 1 + C'(t/t^*)^{1/2} & (t \ll \tau_{\rm fast}) \\ 1 + Q'(\tau_{\rm fill}/t)^{1/2} & (\tau_{\rm fast} \ll t \ll \tau_{\rm slow}) \end{cases} \qquad (v_0 < 0) \tag{34}$$

where Q, Q' are positive constants. Finally, it is straightforward to show that the relaxation for for $t \gg \tau_{\rm slow}$ is exponential as for the stronger perturbations, equation (22).

The most important result of this section is that even though the $\epsilon < \epsilon_{\rm c}$ case is "weak" as compared to Sections 3 and 4, the system's response remains large and nonlinear. One sees from equations (33) and (34) that at $\tau_{\rm fast}$ when the deviation of $\phi_t(0)$ from equilibrium is largest, the relative deviation of $\phi_t(0)$ from equilibrium is much larger than ϵ. Therefore even in the weak case a hole or peak does

form in the MWD but of a smaller amplitude as compared to the stronger perturbation case (see Figs. 13, 14).

Now the dispersion dynamics may be similarly evaluated using equations (33) and (34) in equation (25). One finds that Δ_t relaxes once again on a timescale $\tau_{\rm slow}$. For the positive initial velocity case one finds

$$\delta\Delta_t/\Delta_\infty - \delta\Delta_0/\Delta_\infty \approx \begin{cases} (C/3)(t/\tau_{\rm slow})(t/t^*)^{1/2} & (t \ll \tau_{\rm fast}) \\ Q\epsilon\theta^{-1}(t/\tau_{\rm slow})^{1/2} & (\tau_{\rm fast} \ll t \ll \tau_{\rm slow}) \\ -\delta\Delta_0/\Delta_\infty + (8M/39)\,\epsilon\,(\tau_{\rm slow}/t)^{5/2} e^{-t/(16\tau_{\rm slow})} & \\ & (t \gg \tau_{\rm slow}) \end{cases} \tag{35}$$

while for a negative initial boost

$$\delta\Delta_t/\Delta_\infty - \delta\Delta_0/\Delta_\infty \approx \begin{cases} -(C'/3)(t/\tau_{\rm slow})(t/t^*)^{1/2} & (t \ll \tau_{\rm fast}) \\ -Q'\epsilon\theta^{-1}(t/\tau_{\rm slow})^{1/2} & (\tau_{\rm fill} \ll t \ll \tau_{\rm slow}) \\ -\delta\Delta_0/\Delta_\infty - (8M'/39)\,\epsilon\,(\tau_{\rm slow}/t)^{5/2} e^{-t/(16\tau_{\rm slow})} & \\ & (t \gg \tau_{\rm slow}). \end{cases} \tag{36}$$

7 General perturbations

We have so far considered a specific type of perturbation, namely T-jumps. In this section we consider general perturbations. We will see that almost all of the phenomenology remains unchanged.

Let us start with another simple type of perturbation: addition of a very small amount of monomer to an equilibrated system. (This would require special care to avoid introducing impurities which in current experimental methods are destroyed by the initiators before polymerization [2].) Changing the total amount of monomer perturbs both independent system parameters, r and f (see Eq. (7)), while a T-jump perturbed only f. Despite this, the results of the previous sections remain identical. The reason is that since in both cases the initial MWD is an exponential distribution whose mean is different from the new target equilibrium MWD, the only variable parameterizing the perturbation is $\delta\bar{N}_0$, or equivalently δm_0. Thus one sees from equation (9) that monomer addition is simply equivalent to a positive velocity boost induced by a T-jump.

Consider now the most general perturbation, i.e. one generating an initial MWD of arbitrary shape as shown in Figure 8b. (This should be compared to the T-jump and m-jump which produce initial MWDs of exponential shape with a mean slightly displaced from equilibrium.) Such a general perturbation is small provided

$$\frac{|\delta\phi_0(N)|}{\phi_\infty(N)} \lesssim \epsilon \tag{37}$$

for all N. As for the T-jump case, we have now

$$\epsilon \equiv \frac{\delta m_0}{m_\infty} \approx -\frac{\delta\bar{N}_0}{\bar{N}_\infty}\theta = -\frac{\theta}{\bar{N}_\infty}\int_0^\infty dN\, N\delta\phi_0(N). \tag{38}$$

Since equation (38) is of the same form as equation (9), all the arguments of Section 3 leading to the large relative perturbation in v (Eq. (13)) remain unchanged. Moreover, in our analysis of Sections 3, 4, and 5, the exact shape of the perturbed MWD did not matter in any of the leading order results we obtained. The reason is that the effect of the velocity field on the MWD is so drastic that to first order the response of any MWD close enough to equilibrium is the same, in the sense that the MWD simply translates, creating a hole (or peak). Thus the analysis of Sections 3, 4 and 5 directly apply to the general case.

A special exception is when the first moment of the perturbation $\delta\phi_t(0)$ is arranged to have a value much smaller than $\epsilon\bar{N}_\infty$. In this case the relative amount of monomer-polymer mass transfer is much less than ϵ and this in turn reduces the velocity perturbation. For example, if the first moment were chosen to be so small that $\delta m_0/m_\infty \lesssim 1/\bar{N}_\infty$, then from equation (13) one sees that the relative perturbation in v_t is of order ϵ, much less than the order $\epsilon\bar{N}_\infty$ produced by a T-jump. In such cases, linear response applies for all times. However, if the first moment of $\delta\phi_0$ is much greater than unity the response remains nonlinear.

8 Discussion

The peculiarity of living polymers is that different moments of the MWD relax to equilibrium on different timescales. In the present work we have shown that the first moment, i.e. the mean length, $\bar{N}_t$, relaxes on a timescale $\tau_{\rm fast}$. However the shape of the MWD measured by the second moment, or equivalently the dispersion, Δ_t, relaxes after $\tau_{\rm slow}$. Because the two timescales depend on different powers of $\bar{N}_\infty$ their ratio may be extremely large:

$$\tau_{\rm fast} \approx \frac{\bar{N}_\infty}{v^-}\frac{f}{(1-f)}, \qquad \tau_{\rm slow} \approx \frac{\bar{N}_\infty^2}{4v^-}, \tag{39}$$

where $1/v^-$ is the natural time scale and $f \approx m_\infty/m_{\rm tot}$ is approximately the fraction of non-polymerized monomer. Our only assumption has been that f is not extremely close to unity, i.e. the system is not very close to the polymerization temperature.

In addition to the MWD, the other important observable is the free monomer concentration, m_t. We emphasize that since the number of chains is fixed by the number of initiators, thus m_t is linearly coupled to $\bar{N}_t$ by mass conservation for all times. Hence the relaxation of these two quantities is identical and m_t relaxes after $\tau_{\rm fast}$. Note that for certain other living polymers such as end-polymerizing wormlike surfactant micelles, this is not true [29,30,55]. In these systems there is no separate initiator species and a pair of monomers may spontaneously unite to form a living chain. The dynamics are thus very different and m_t and $\bar{N}_t$ may relax on different timescales. Marques et al. [29] studied this class of living polymer; after linearizing dynamical equations they found that after a small T-jump m_t relaxes much more rapidly than $\bar{N}_t$ which subsequently relaxes in time $\sim \bar{N}_\infty^2$. In numerical simulations of this

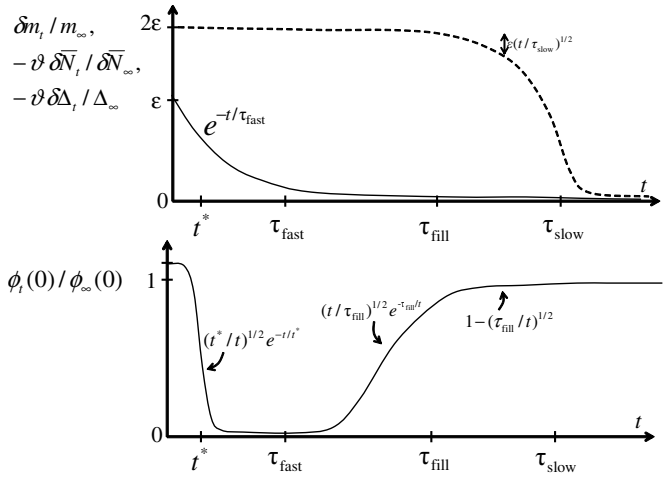

Fig. 15. Time dependent recovery following a small perturbation, positive initial boost, $\epsilon > \epsilon_c$. Top: $\delta\bar{N}_t$, δm_t (solid line) become very small after τ_{fast} while the MWD dispersion $\delta\Delta_t$ (dashed line) relaxes after τ_{slow}. Bottom: In the process of equilibration free initiator concentration undergoes large changes even though its initial and equilibrium values are very close to one another.

same class of system, Milchev et al. [30] report a $1/t$ decay of mean chain length after a time $\sim \bar{N}_\infty^5$. In the related system of spherical micelle aggregation [56–59], the number of micelles can change and again the kinetics are very different [54] to the present case.

A summary of our findings is shown in Figure 15, for the case emphasized here where a small T-jump induces a positive velocity boost to chain growth. The figure shows the very different relaxation times of first and second MWD moments. It also shows the interesting behavior of the number of free initiators, $\phi_t(0)$, which suffers enormous depletion at intermediate times despite ultimately recovering to a level very close to its initial value. We showed that whilst virtually all of the relaxation of the fast variables $\bar{N}_t, m_t$ occurs on a timescale τ_{fast}, they are actually not completely relaxed by this time. The final very late stages of their relaxation during which their values are fine-tuned (to relative order $1/\bar{N}_\infty$) to the final equilibrium values, occurs on a timescale τ_{slow}. During this episode their values evolve quasi-statically, enslaved to $\phi_t(0)$ according to $\delta\bar{N}_t\theta/\bar{N}_\infty \approx -\delta m_t/m_\infty \approx \delta\phi_t(0)$. The novel behavior of $\phi_t(0)$, as well as its central role in late relaxation of the fast variables suggests this as an interesting quantity to measure experimentally. This might be achieved spectroscopically and would have the advantage of being a relatively uninvasive probe. We remark that for bifunctional initiators, e.g. those used in studies by the Greer group, the meaning of $\phi_t(0)$ is the concentration of "half-chains," i.e. those having at least one chain end which is a bare initiator molecule.

We have demonstrated that the type of dynamical response depends on the magnitude and sign of the perturbation. For example, if the temperature change is reversed in sign, then the velocity boost also changes sign. Thus for α-methylstyrene a negative T-jump produces the positive velocity boost phenomenology of Figure 15 whereas a small temperature increase causes a negative boost. In this case, instead of short chains being annihilated, their number increases dramatically during the relaxation process. As far as perturbation magnitude is concerned, if the relative value ϵ is less than a critical value $\sim 1/\bar{N}_\infty^{1/2}$ then the response is milder but remains non-linear. For a positive boost, the hole in the MWD is no longer complete, but instead has a relative depth less than unity but still much bigger than ϵ.

How do our predictions compare with experiment? In reference [11] small T-jumps were imposed on α-methylstyrene systems in the semi-dilute regime at concentrations high enough to be nearly entangled. Relaxation was monitored by measuring viscosity η as a function of time. Now generally we expect viscosity to scale as a polymer-concentration-dependent power of mean chain length, $\eta \sim c_\phi \bar{N}^\gamma$, where the value of γ is predicted by standard theories of polymer physics [47,60]. For a general MWD, note the coefficient c_ϕ which depends on the shape of the MWD, i.e. it depends on the full function $[\phi(N)]$. (This is because η depends not only on the first moment, but in general has a complex dependence on chain length distribution.) Thus we predict an initial fast relaxation of η lasting time $\tau_{fast} = \bar{N}/(\theta v^-)$ (corresponding to the relaxation of $\bar{N}$) followed by a much slower relaxation in τ_{slow} (this is the relaxation of the prefactor c_ϕ). The fast relaxation time is independent of T-jump magnitude (i.e. independent of ϵ). Now from equations (6) and (7) we can rewrite $\tau_{fast} = 1/(rk^+ m_{tot})$. Using [11] $r = 4.7 \times 10^{-4}$, $m_{tot} = 0.29$ gm/cm^3 and a measured value [12] $k^+ \approx 0.2M^{-1}$ s^{-1} one estimates $\tau_{fast} \approx 1000$ s. (Note that this work involved bifunctional initiators. In reference [54] we incorrectly estimated τ_{fast} to be twice the value calculated here based on a wrong estimate of the number of living chains which was taken to be equal to the number of bifunctional initiators instead of twice this value.) Similarly, with [2] $f \approx 0.5$, $v^- = 0.1$ s^{-1} one finds $\tau_{slow} \approx 1$ month. Hence for these experiments (timescales much less than months) η should relax in approximately 1000 s. In the experiments, jumps $\delta T \approx 1$ °C were imposed at various temperatures in the range 283 °K $\lesssim T \lesssim$ 290 °K. Now the temperature dependence of $\tau_{fast} \sim 1/k^+$ is determined by k^+ which is reported [12] to vary by $\approx 10\%$ over this temperature range. Thus we expect only a slight variation in the viscosity relaxation time at the different temperatures studied (despite the fact that $\bar{N}_\infty$ changes significantly). These predictions are very close to the experimental findings, where relaxation times at all temperatures were found to be about 2000 seconds, with very little variation from one temperature to another. This is in sharp contrast to the relative changes in η itself, which varied by almost an order of magnitude.

We have emphasized small perturbations in this work. In fact, the response to a large perturbation is obtained, qualitatively speaking, by setting $\epsilon = 1$ in our results. This case was addressed by Miyake and Stockmayer [44] who considered an initial condition in which all initiators are

free (i.e. $\bar{N}_0 = 0$). They were the first to identify the two timescales of the system, $\tau_{\rm fast}$ and $\tau_{\rm slow}$, in the limit of very small depolymerization rates ($f \ll 1$). Their analytical results applied to the $t < \tau_{\rm fast}$ stage where they found an initially uniformly translating and broadening MWD peak, reaching $\bar{N}_\infty$ after $\tau_{\rm fast}$ as shown in Figure 5. Seen from the viewpoint of a general perturbation of magnitude ϵ, in this case $\tau_{\rm fill}$ and $\tau_{\rm slow}$ coincide because $\epsilon = 1$. That is, the "hole" (in this case the entire region between 0 and $\bar{N}_\infty$) fills up on the same timescale in which the whole MWD relaxes. The linearized dynamics, which for a small perturbation applied for $t > \tau_{\rm fill}$ due to $\delta\phi_t(0)/\phi_\infty(0)$ becoming small (see Sect. 3.3) cannot be employed. Describing dynamics at times of order $\tau_{\rm slow}$ in this case is thus a difficult nonlinear problem [51–53].

In recent experiments, Greer's group [12,13] studied such large perturbations using α-methylstyrene. After a rapid quench below the polymerization temperature, monomer concentration and MWD were analyzed after a time delay. The time dependent relaxation was probed by repeating the procedure for different time delays and samples. They found different relaxation times for the monomer concentration and the MWD width, as predicted by theory [44]. However, $\bar{N}_t$ and m_t did not have the same relaxation, as mass conservation would seem to dictate. This may be due either to side-reactions during polymerization or living chain ionic association effects [61–63] which have been studied theoretically [25]. Dynamic light scattering measurements [64] suggest that prior to polymerization the initiators self-assemble into long polymeric structures and it has been suggested [13] that initiators may not all be equally available for polymerization following the T-quench. However, lifetimes of aggregate structures would need to be extremely long for these effects to interfere with polymerization dynamics since as we have seen the MWD relaxation times are very large.

In conclusion, our hope is that this work will motivate further experimental study of the dynamical sensitivity of living polymers to small perturbations. The drastic effect on the MWD in the small chain region, in particular the depletion or excess of free initiators, is a natural focus for experimental measurement. One can think of other *time-dependent* perturbations such as small amplitude thermal cycling which would probe interesting aspects of their ultrasensitive dynamics. Finally, the systems we have analyzed here are model starting points for the considerably more complex biological living polymers, actin filaments and microtubules, which are intimately involved in the locomotion and structural integrity of living cells [39–41].

This work was supported by the Petroleum Research Fund, grant No. PRF-33944-AC7.

Appendix A: Derivation of equilibrium values m_∞, $\bar{N}_\infty$, v_∞, D_∞

The equilibrium MWD can be calculated by setting the time derivative in equation (5) to zero. Its solution is the Flory distribution, equation (1), where

$$\bar{N}_\infty = -D_\infty / v_\infty. \tag{40}$$

Solving the system of equations (40) and (2) for $m_\infty, \bar{N}_\infty$ one has

$$\frac{m_\infty}{m_{\rm tot}} = \frac{1}{2}\left\{1+f+\frac{r}{2}-\left[(1-f)^2+r(1+3f)+\frac{r^2}{4}\right]^{1/2}\right\}$$
$$\bar{N}_\infty = \frac{1}{r}\left(1-\frac{m_\infty}{m_{\rm tot}}\right). \tag{41}$$

For $r \ll 1$ and assuming $(1-f)/r^{1/2} \gg 1$, by expanding equation (41) in powers of r and keeping only the first term of the expansion one recovers equation (8). The values of v_∞, D_∞ in equation (8) are obtained by substitution of $m_\infty, \bar{N}_\infty$ in equation (4).

Appendix B: Self-consistency of results of Sections 3.1 and 3.2

B.1 Coherent chain growth

The solution for the v_t dynamics, equation (14), follows by solving equation (6) after neglecting the $\phi_t(0)$ term on the rhs. For $t \ll \tau_{\rm qs}$, this is a self-consistent solution since then the $\phi_t(0)$ term is negligible with respect to the remaining terms as can be seen using the solutions for $v_t, \phi_t(0)$ of equations (14, 17), and (21).

Equation (15) is derived by substituting v_t from equation (14) in equation (5), replacing $D_t = D_\infty + \delta D_t$, and dropping the δD_t term. The fact that this term can be neglected may be seen as follows. Even if δD_t did not decrease but remained of order δD_0 throughout this regime this would lead to replacing D_∞ by $D_\infty(1+\epsilon)$ in all results obtained in Section 3 (see Eq. (13)). This upper bound on the effect of δD_t can easily be seen to lead to higher order in ϵ terms (see e.g. Eq. (17)) and the δD_t term can therefore be neglected.

Now let us consider the propagator of the dynamics of equation (15), which appears in equation (16). For short times, $t \ll \tau_{\rm fast}$, one may replace v_t in equation (15) by v_0. Equation (15) then has constant coefficients and its propagator including the boundary condition may be calculated exactly [38]:

$$G_t^{\rm tran}(N,N') = \frac{1}{(4\pi D_\infty t)^{1/2}}\left\{e^{-(N-N'-v_0 t)^2/(4D_\infty t)} + e^{-N'v_0/D_\infty} e^{-(N+N'-v_0 t)^2/(4D_\infty t)}\right\}$$
$$- \frac{v_0}{2D_\infty} e^{Nv_0/D_\infty} \mathrm{erfc}\left(\frac{N+N'+v_0 t}{(4D_\infty t)^{1/2}}\right) \quad (t \ll \tau_{\rm fast}). \tag{42}$$

Here $\mathrm{erfc}(x) \equiv 1 - \mathrm{erf}(x)$, where erf is the error function.

The solution for $\phi_t(0)$ is derived by substituting equation (42) in equation (16) and setting $N = 0$. One has

$$\frac{\phi_t(0)}{\phi_\infty(0)} \approx \mathrm{erfc}(x) + 2x^2 \mathrm{erfc}(x) - 2\pi^{-1/2} x e^{-x^2},$$
$$x \equiv (t/t^*)^{1/2} \qquad (t \ll \tau_{\rm fast}). \tag{43}$$

Here we used the fact that since the values of N' contributing to the integration are much smaller than $\bar{N}_\infty$, one may approximate $\phi_0(N')$ by $\phi_\infty(0)$ in the integrand of equation (16) (with relative errors of order $1/\bar{N}_\infty$). Equation (17) of the main text follows from equation (43) by taking the two corresponding limits. Note that equation (43) approximates $\phi_t(0)$ for all $t \ll \tau_{\rm fast}$, including times of order t^*.

B.2 Hole filling

Equation (18) is a self-consistent solution of equation (6) since for $t \gg \tau_{\rm qs}$, assuming the validity of equations (18) and (17) one may verify that equation (6) is satisfied with the term on the lhs being much smaller in magnitude than both terms on the rhs which balance one another.

Consider now the validity of equation (19) for $\tau_{\rm fast} \ll t \ll \tau_{\rm fill}$. Substituting equation (21) into equation (18) one has explicit solutions for $m_t, \bar{N}_t, v_t, D_t$. One thus sees that in the time regime of consideration the velocity term in equation (5) is exponentially small and therefore can be deleted in equation (19) with very small error.

The MWD dynamics are therefore described by equation (19) whose propagator satisfying reflecting boundary conditions is

$$G_t^{\rm diff}(N,N') = \frac{1}{(4\pi D_\infty t)^{1/2}} \times \left\{ e^{-(N-N')^2/(4D_\infty t)} + e^{-(N+N')^2/(4D_\infty t)} \right\}. \quad (44)$$

The solution of equation (19) is thus

$$\begin{aligned}\phi_t(N) &\approx \int_0^\infty dN'\, \phi_{t_{\rm cross}}(N') G^{\rm diff}_{t-t_{\rm cross}}(N,N') \\ &\approx \int_{\epsilon\bar{N}_\infty/\theta}^\infty dN'\, \phi_0(N' - \epsilon\bar{N}_\infty/\theta) G_t^{\rm diff}(N,N') \\ &\quad (\tau_{\rm fast} \ll t \ll \tau_{\rm fill}). \end{aligned} \quad (45)$$

where $t_{\rm cross}$ satisfies $\tau_{\rm fast} \ll t_{\rm cross} \ll \tau_{\rm qs}$, i.e. it belongs to the time regime described simultaneously by equations (15) and (19). In going from the first integral in equation (45) to the second we used the fact that at $t_{\rm cross}$ the MWD has approximately the shape of the initial MWD, boosted in the positive direction by $\epsilon\bar{N}_\infty/\theta$. The effect of diffusion during the initial boost of the MWD may be shown to be small. Notice also that evolution in the last expression in equation (45) starts at $t = 0$; for $t \gg t_{\rm cross}$ we may to leading order replace $t - t_{\rm cross}$ in $G^{\rm diff}$ in equation (45) by t.

Substituting equation (44) in equation (45) and setting $N = 0$ one obtains

$$\frac{\phi_t(0)}{\phi_\infty(0)} \approx {\rm erfc}\left[\left(\frac{\tau_{\rm fill}}{t} \right)^{1/2} \right], \quad (\tau_{\rm fast} \ll t \ll \tau_{\rm fill}) \quad (46)$$

Considering times much shorter than the crossover time $\tau_{\rm fill}$, equation (21) is recovered.

Appendix C: Linearized dynamics, $t \gg \tau_{\rm fill}$

Ultrasensitivity is such that the dynamics cannot be linearized until the later stages, $t \gg \tau_{\rm fill}$. For these times we may linearize equation (5) by dropping terms proportional to products of $\delta\phi_t, \delta v_t, \delta D_t$. One has

$$\begin{aligned}\frac{\partial \delta\phi_t}{\partial t} &\approx -v_\infty \frac{\partial \delta\phi_t}{\partial N} + D_\infty \frac{\partial^2 \delta\phi_t}{\partial N^2} + \mu_t, \\ \mu_t &\equiv \frac{\delta v_t}{\bar{N}_\infty} \left[\phi_\infty(N) - \delta(N) \right], \end{aligned} \quad (47)$$

with reflecting boundary conditions at the origin. In equation (47) the δD_t term was neglected since its magnitude is smaller by $1/\bar{N}_\infty$ than the corresponding δv_t term. The δ-function in the source term in equation (47) arises from linearizing the boundary condition in equation (5). Notice that by definition, $\delta\phi_t(0)$ is normalized to zero and that the source term in equation (47) preserves this normalization since its integral over all N is zero.

Performing the corresponding linearization in equation (6) one has

$$\frac{d}{dt}\delta v_t \approx -\frac{1}{\tau_{\rm fast}}\delta v_t - \frac{1}{\tau_{\rm fast}} D_\infty \delta\phi_t(0). \quad (48)$$

Now since equation (47) is of the same form as equation (15), its propagator, $G_t^{\rm linear}(N,N')$, is given by equation (42) with v_0 replaced by v_∞. Thus if $\delta\phi_{t_L}(N)$ is known at time t_L, then the solution of equation (47) for subsequent times is

$$\delta\phi_t(N) \approx \int_0^\infty dN'\, G^{\rm linear}_{t-t_L}(N,N') \delta\phi_{t_L}(N') + R_t(N), \quad (49)$$

where

$$\begin{aligned} R_t(N) &\equiv \int_0^\infty dN' \int_{t_L}^t dt'\, G^{\rm linear}_{t-t'}(N,N') \mu_{t'}(N') \\ &\approx -\int_{t_L}^t dt'\, \frac{D_\infty \delta\phi_t(0)}{\bar{N}_\infty} [\phi_\infty(N) - G^{\rm linear}_{t-t'}(N,0)]. \end{aligned} \quad (50)$$

Here the last expression for $R_t(N)$ is obtained by performing the N' integration using the expression for μ_t from equation (47) and the fact that $\phi_\infty(N)$ remains unchanged when evolved with $G^{\rm linear}$. In equation (50) we also used

$$\delta v_t \approx -D_\infty \delta\phi_t(0) \quad (51)$$

which is valid throughout the linearized time regime as one may derive using equation (48). The solution of equations (47) and (48) is thus found by setting $N = 0$ in equation (49), solving for $\delta\phi_t(0)$, and then using the calculated expression in equations (49) and (51) to find $\delta\phi_t(N)$ and δv_t. Let us now perform this analysis for two time regimes.

(i) $\tau_{\rm fill} \ll t \ll \tau_{\rm slow}$. In this regime, we will see the source term can in effect be ignored. The top expression on the rhs of equation (22) is a self-consistent solution of equation (49) which is proved as follows. As one may see from equations (21) and (22) there exists a constant

β of order unity such that for $t > \beta\tau_{\rm fill}$ the relative perturbation in $\phi_t(N)$ is much smaller than unity and equation (47) applies. (More precisely, for any desired relative smallness there exists a different constant β.) Thus setting $t_L = \beta\tau_{\rm fill}$ and $N = 0$ in equation (49) and using the expression for $\delta\phi_t(0)$ from equation (22) one finds that with appropriate choice of J, equation (49) is satisfied with $R_t(0)$ being much smaller than the remaining two terms in equation (49). The integral term in equation (49) is calculated using the fact that as seen from equations (21, 22), and Figure 10, $\delta\phi_{t_L}(N)$ is of order $\delta\phi_{t_L}(0) \gg \epsilon\phi_\infty(N)$ for $N \ll \epsilon\bar{N}_\infty/\theta$ and of order $\epsilon\phi_\infty(N)$ for larger N. We also used

$$G^{\rm linear}_{t-t'}(0,N') \rightarrow \begin{cases} 1/\left[D_\infty(t-t')\right]^{1/2} & (N' \ll D_\infty(t-t')) \\ 0 & (N' \gg D_\infty(t-t')) \end{cases} \quad (t,t' \ll \tau_{\rm slow}) \quad (52)$$

which may be derived from equation (42).

(ii) $t \gg \tau_{\rm slow}$. Using equation (42) one finds

$$G^{\rm linear}_t(0,N') \approx S_\infty + (S_t - S_\infty)\,\lambda(N') \quad (t \gg \tau_{\rm slow}), \quad (53)$$

where

$$S_t \equiv G^{\rm linear}_t(0,0),\ S_\infty = \phi_\infty(0) = 1/\bar{N}_\infty, \qquad \lambda(N') \equiv \left(1 - \frac{N'}{2\bar{N}_\infty}\right) e^{N'/(2\bar{N}_\infty)}. \quad (54)$$

Now setting $t_L = \tau_{\rm slow}$ in equation (49) and using equations (50) and (53) one has

$$\delta\phi_t(0) \approx (S_t - S_\infty) \int_0^\infty dN'\,\lambda(N')\delta\phi_{\tau_{\rm slow}}(N') + \frac{1}{4S_\infty\tau_{\rm slow}} \int_{\tau_{\rm slow}}^t dt'\,(S_{t-t'} - S_\infty)\,\delta\phi_{t'}(0) \quad (55)$$

where we used the fact that $\delta\phi_{\tau_{\rm slow}}(N')$ is normalized to zero.

Now the self-consistency of the $t > \tau_{\rm slow}$ expression on the rhs of equation (22) is proved by substituting equation (22) in equation (55). Since $\delta\phi_{\tau_{\rm slow}}(N')$ is of order $\epsilon/\bar{N}_\infty$, the magnitude of the integral of $\delta\phi_{\tau_{\rm slow}}(N')$ in equation (55) is of order ϵ. The last integral term in equation (55) is evaluated using equation (22) and

$$S_t - S_\infty \approx \begin{cases} 1/(D_\infty t)^{1/2} & (t \ll \tau_{\rm slow}) \\ 16 S_\infty \pi^{-1/2}\,(\tau_{\rm slow}/t)^{3/2}\,e^{-t/(16\tau_{\rm slow})} & (t \gg \tau_{\rm slow}) \end{cases} \quad (56)$$

which may be proved using equations (54) and (42). One finds that for $t \gg \tau_{\rm slow}$ all terms in equation (55) have the same time dependence and are of the same order of magnitude. Thus equation (55) may be satisfied by appropriate choice of the numerical coefficient M in equation (22).

Appendix D: Self-consistency of the results of Section 5

D.1 Coherent chain shrinking

The validity of equation (14) is verified using the same arguments as in the first paragraph of Appendix B but now using the expression for $\phi_t(0)$ from equation (28).

Setting $N = 0$ in equation (45) one obtains equation (43) with x now replaced by $-x$. Considering times much greater and much less than t^* leads to equation (28).

D.2 Peak decay

The validity of equation (18) is proved using exactly the same arguments as the ones in the first paragraph of the corresponding section of Appendix B, but now using the expression for $\phi_t(0)$ from equation (29). One finds that the crossover time $\tau_{\rm qs} \approx \tau_{\rm fast}\ln(\bar{N}_\infty)$ is different from the respective crossover time found in Appendix B.

The solution of equation (19) is now

$$\phi_t(N) \approx \int_0^\infty dN'\,\phi_0(N' - \epsilon\bar{N}_\infty/\theta)G^{\rm diff}_t(N,N') + G^{\rm diff}_t(N,0)\int_0^{\epsilon\bar{N}_\infty/\theta} dN'\,\phi_0(N')\ (\tau_{\rm fast} \ll t \ll \tau_{\rm slow}). \quad (57)$$

Here the evolved MWD consists of two parts, corresponding to the two terms on the rhs (see Fig. 11c). The first is the initial MWD, ϕ_0, shifted by $\epsilon\bar{N}_\infty/\theta$ towards smaller N. The second part is the excess peak accumulated by the negative boost at the origin and whose amount was the polymer initially lying between zero and $\epsilon\bar{N}_\infty/\theta$. Here, as in Section 3, the effects of diffusive broadening during $t < \tau_{\rm fast}$ have been neglected, and $\tau_{\rm fast}$ in equation (57) has been replaced by zero.

Now substituting equation (44) in equation (57) and setting $N = 0$ one obtains equation (29) similarly to the derivation of equation (21) in Appendix B.

Appendix E: Self-consistency of the results of Section 6

For times $t \ll \tau_{\rm fast}$, all results and analysis are identical to those for the strong perturbation ($\epsilon > \epsilon_{\rm c}$) case in the regime $t \ll t^*$. Equation (32) can be shown to be a self-consistent solution using the same arguments as those of Appendices B and D to prove equations (14) and (18), respectively. For times longer than $\tau_{\rm fast}$ linearization of the dynamics can be performed and the results of Appendix C directly apply.

References

1. M. Szwarc, M. Van Beylen, *Ionic Polymerization and Living Polymers* (Chapman and Hall, New York, 1993)
2. S.C. Greer, Adv. Chem. Phys. **XCIV**, 261 (1996)
3. S.C. Greer, Ann. Rev. Phys. Chem. **53**, 173 (2002)
4. S.C. Greer, J. Phys. Chem. B **102**, 5413 (1998)
5. K.M. Zheng, S.C. Greer, Macromolecules **25**, 6128 (1992)
6. K.M. Zheng, S.C. Greer, L.R. Corrales, J. Ruiz-Garcia, J. Chem. Phys. **98**, 9873 (1993)
7. A. Ploplis Andrews, K.P. Andrews, S.C. Greer, F. Boué, P. Pfeuty, Macromolecules **27**, 3902 (1994)
8. S. Sarkar Das, A. Ploplis Andrews, S.C. Greer, J. Chem. Phys. **102**, 2951 (1995)
9. J. Zhuang, A. Ploplis Andrews, S.C. Greer, J. Chem. Phys. **107**, 4705 (1997)
10. P. Pfeuty, F. Boué, J.P. Ambroise, R. Bellissent, K.M. Zheng, S.C. Greer, Macromolecules **25**, 5539 (1992)
11. J. Ruiz-Garcia, S.C. Greer, J. Molecular Liquids **71**, 209 (1997)
12. J. Zhuang, S.S. Das, M.D. Nowakowski, S.C. Greer, Physica A **244**, 522 (1997)
13. S. Sarkar Das, J. Zhuang, A. Ploplis Andrews, S.C. Greer, C.M. Guttman, W. Blair, J. Chem. Phys. **111**, 9406 (1999)
14. S.J. Kennedy, J.C. Wheeler, J. Chem. Phys. **78**, 953 (1980)
15. J.C. Wheeler, S.J. Kennedy, P.M. Pfeuty, Phys. Rev. Lett. **45**, 1748 (1980)
16. J.C. Wheeler, P.M. Pfeuty, Phys. Rev. A **24**, 1050 (1981)
17. J.C. Wheeler, P.M. Pfeuty, Phys. Rev. Lett. **71**, 1653 (1993)
18. L. Schafer, Phys. Rev. B **46**, 6061 (1992)
19. M. Kaufman, Phys. Rev. B **39**, 6898 (1989)
20. J.C. Wheeler, R.G. Petschek, Phys. Rev. B **45**, 171 (1992)
21. J. Dudowicz, K.F. Freed, J.F. Douglas, J. Chem. Phys. **111**, 7116 (1999)
22. J. Dudowicz, K.F. Freed, J.F. Douglas, J. Chem. Phys. **112**, 1002 (2000)
23. J. Dudowicz, K.F. Freed, J.F. Douglas, J. Chem. Phys. **113**, 434 (2000)
24. P. van der Schoot, Macromolecules **35**, 2845 (2002)
25. A.L. Frischknecht, S.T. Milner, J. Chem. Phys. **114**, 1032 (2001)
26. O.W. Webster, Science **251**, 887 (1991)
27. C.C. Hawker, Acc. Chem. Res. **30**, 373 (1997)
28. M.K. Georges, P.P.N. Veregin, P.M. Kazmaier, G.K. Hamer, Macromolecules **26**, 2987 (1993)
29. C.M. Marques, M.S. Turner, M.E. Cates, J. Chem. Phys. **99**, 7260 (1996)
30. A. Milchev, Y. Rouault, D.P. Landau, Phys. Rev. E **56**, 1946 (1997)
31. C.M. Marques, M.E. Cates, J. Phys. II France **1**, 489 (1991)
32. M.E. Cates, S.F. Candau, J. Phys.: Condens. Matter **2**, 6869 (1990)
33. J.P. Wittmer, A. Milchev, M.E. Cates, J. Chem. Phys. **109**, 834 (1998)
34. J.P. Wittmer, A. Milchev, M.E. Cates, Europhys. Lett. **41**, 291 (1998)
35. N.A. Spenley, M.E. Cates, T.C.B. McLeish, Phys. Rev. Lett. **71**, 939 (1993)
36. B. O'Shaughnessy, J. Yu, Phys. Rev. Lett. **74**, 4329 (1995)
37. F. Oosawa, S. Asakura, *Thermodynamics of the Polymerization of Protein* (Academic Press, New York, 1975)
38. T.L. Hill, *Linear Aggregation Theory in Cell Biology* (Springer Verlag, New York, 1987)
39. E.D. Korn, M.-F. Carlier, D. Pantaloni, Science **238**, 638 (1987)
40. T.D. Pollard, J.A. Cooper, Ann. Rev. Biochem. **55**, 987 (1986)
41. A. Desai, T.J. Mitchison, Annu. Rev. Cell Dev. Biol. **13**, 83 (1997)
42. H. Flyvbjerg, T.E. Holy, S. Leibler, Phys. Rev. Lett. **73**, 2372 (1994)
43. B. O'Shaughnessy, Q. Yang, D. Vavylonis (manuscript in preparation)
44. A. Miyake, W.H. Stockmayer, Die Makromolekulare Chemie **8**, 90 (1965)
45. P. Flory, *Principles of Polymer Chemistry* (Cornell University Press, Ithaca, New York, 1971)
46. A.V. Tobolsky, A. Rembaum, A. Eisenberg, J. Polym. Sci. **45**, 347 (1960)
47. P.G. de Gennes, *Scaling Concepts in Polymer Physics* (Cornell Univ. Press, Ithaca, New York, 1985)
48. J. des Cloizeaux, G. Jannink, *Polymers in Solution, Their Modelling and Structure* (Clarendon Press, Oxford, 1990)
49. J. des Cloizeaux, J. Phys. (France) **36**, 281 (1975)
50. W.B. Brown, M. Szwarc, Trans. Far. Soc. **54**, 416 (1958)
51. V.S. Nanda, S.C. Jain, Eur. Pol. J. **6**, 1517 (1970)
52. F.C. Auluck, G.C. Gupta, V.S. Nanda, Pramana J. Phys. **27**, 43 (1986)
53. N.G. Taganov, Sov. J. Chem. Phys. **1**, 2329 (1984)
54. B. O'Shaughnessy, D. Vavylonis, Phys. Rev. Lett. **90**, 118301 (2003)
55. J.D. Wattis, J.R. King, J. Phys. A **31**, 7169 (1998)
56. E.A.G. Aniansson, S.N. Wall, J. Phys. Chem. **78**, 1024 (1974)
57. E.A.G. Aniansson, S.N. Wall, J. Phys. Chem. **79**, 857 (1975)
58. E.A.G. Aniansson et al., J. Phys. Chem. **80**, 905 (1976)
59. H. Wennerstrom, B. Lindman, Phys. Rep. **52**, 1 (1979)
60. M. Doi, S.F. Edwards, *The Theory of Polymer Dynamics* (Clarendon Press, Oxford, 1986)
61. L.J. Fetters, N.P. Balsara, J.S. Huang, H.S. Heong, K. Amdal, M.Y. Lin, Macromolecules **28**, 4996 (1995)
62. J. Stellbrink, L. Willner, O. Jucknischke, D. Richter, P. Lindner, L.J. Fetters, J.S. Huang, Macromolecules **31**, 4189 (1998)
63. N.P. Balsara, L.J. Fetters, Macromolecules **32**, 5147 (1999)
64. J. Ruiz-Garcia, R. Castillo, J. Chem. Phys. **110**, 10657 (1999)